Cell Death and Differentiation (2012) 19, 947–957

www.nature.com/cdd

Transfer of IP_3 through gap junctions is critical, but not sufficient, for the spread of apoptosis

E Decrock[1,11], DV Krysko[2,3,12], M Vinken[4,12], A Kaczmarek[2,3,11], G Crispino[5], M Bol[1], N Wang[1], M De Bock[1], E De Vuyst[1], CC Naus[6], V Rogiers[4], P Vandenabeele[2,3], C Erneux[7], F Mammano[5,8,9], G Bultynck[10] and L Leybaert*[,1]

Decades of research have indicated that gap junction channels contribute to the propagation of apoptosis between neighboring cells. Inositol 1,4,5-trisphosphate (IP_3) has been proposed as the responsible molecule conveying the apoptotic message, although conclusive results are still missing. We investigated the role of IP_3 in a model of gap junction-mediated spreading of cytochrome *C*-induced apoptosis. We used targeted loading of high-molecular-weight agents interfering with the IP_3 signaling cascade in the apoptosis trigger zone and cell death communication zone of C6-glioma cells heterologously expressing connexin (Cx)43 or Cx26. Blocking IP_3 receptors or stimulating IP_3 degradation both diminished the propagation of apoptosis. Apoptosis spread was also reduced in cells expressing mutant Cx26, which forms gap junctions with an impaired IP_3 permeability. However, IP_3 by itself was not able to induce cell death, but only potentiated cell death propagation when the apoptosis trigger was applied. We conclude that IP_3 is a key necessary messenger for communicating apoptotic cell death *via* gap junctions, but needs to team up with other factors to become a fully pro-apoptotic messenger.
Cell Death and Differentiation (2012) **19,** 947–957; doi:10.1038/cdd.2011.176; published online 25 November 2011

Ca^{2+} regulates a wide range of cellular processes, including cell death by apoptosis. It is highly compartmentalized in the cell and alterations in Ca^{2+} distribution induce and control apoptosis.[1–3] The endoplasmic reticulum (ER) is the main intracellular Ca^{2+} store, and is critically involved in intracellular Ca^{2+} homeostasis and signaling. In many cases, pro-apoptotic Ca^{2+} elevation is mediated by inositol 1,4,5-trisphosphate (IP_3)-induced channel opening with rapid mobilization of Ca^{2+} from the ER lumen into the cytosol.[3,4] IP_3-linked Ca^{2+} signals may in turn trigger apoptosis by compromising mitochondrial function.[1,5] Ca^{2+} changes in a cell can be divided into different categories depending on the duration (transient *versus* sustained) or the pattern (oscillations *versus* waves) with sustained Ca^{2+} elevation resulting in cell death, while Ca^{2+} oscillations (repetitive spikes) are suggested to promote cell survival.[6,7] Ca^{2+} signals can also be propagated from cell-to-cell as intercellular Ca^{2+} waves, based on both paracrine signaling and the diffusion of IP_3 *via* gap junction channels (GJs).[6,8]

GJs are constructed by two opposing hemichannels, belonging to the membranes of adjacent cells. Hemichannels are composed of six transmembrane connexin (Cx) proteins, named according to their predicted molecular weight.[9] GJs allow the passage of small and hydrophilic molecules (<1.5 kDa) between the cytoplasm of neighboring cells, which provides them not only important physiological but also pathological functions. Moreover, GJs can control cell death/survival by mediating the spread of pro- and anti-apoptotic molecules between cells.[10] Previous work from our group as well as others demonstrated that cytochrome C (Cyt*C*)-induced apoptosis propagates from dying to healthy neighboring cells through GJs.[11–16] Further investigations toward the biochemical nature of the cell death messenger revealed that Ca^{2+} seems to play a pivotal role in this process.[11,13,16,17] However, slowly mobile cytoplasmic Ca^{2+}-binding proteins limit Ca^{2+} diffusion in the cytoplasm, making IP_3 (MW 420 Da), with a 20 times larger diffusion coefficient and 100 times larger

[1]Department of Basic Medical Sciences – Physiology group, Faculty of Medicine and Health Sciences, Ghent University, Ghent 9000, Belgium; [2]Molecular Signalling and Cell Death Unit, Department for Molecular Biomedical Research, VIB, Ghent 9052, Belgium; [3]Department of Biomedical Molecular Biology, Ghent University, Ghent 9052, Belgium; [4]Department of Toxicology – Center for Pharmaceutical Research, Faculty of Medicine and Pharmacy, Vrije Universiteit Brussel, Brussels 1090, Belgium; [5]Istituto Veneto di Medicina Molecolare, Fondazione per la Ricerca Biomedica Avanzata, Padova 35129, Italy; [6]Department of Cellular and Physiological Sciences, Faculty of Medicine, University of British Columbia, Vancouver, BC, V6 T 1Z3, Canada; [7]Institut de Recherche Interdisciplinaire et Biologie Humaine et Moléculaire (IRIBHM), Faculty of Medicine, Université Libre de Bruxelles, Brussels 1070, Belgium; [8]Dipartimento di Fisica 'G Galilei', Universita' di Padova, Padova 35131, Italy; [9]Istituto CNR di Neuroscienze, Padova, Italy and [10]Department of Molecular Cell Biology-Laboratory of Molecular and Cellular Signalling, Faculty of Medicine, Katholieke Universiteit Leuven, Leuven 3000, Belgium

*Corresponding author: L Leybaert, Department Basic Medical Sciences – Physiology group, Faculty of Medicine and Health Sciences, Ghent University, De Pintelaan 185 (Block B, third floor), Ghent 9000, Belgium. Tel: +32 9 332 33 66; Fax: +32 9 332 30 59; E-mail: Luc.Leybaert@Ugent.be

[11]ED and AK are doctoral research fellows of the Fund for Scientific Research Flanders (FWO-Vlaanderen), Belgium

[12]MV and DVK are postdoctoral research fellows of the Fund for Scientific Research Flanders (FWO-Vlaanderen), Belgium

Keywords: apoptosis; calcium; connexin; inositol 1,4,5-trisphosphate; gap junction

Abbreviations: AI, apoptotic index; AUC, area under the curve; BH4-Bcl-2, BH4 domain of Bcl-2; BIND, a mutant BH4-Bcl-2 peptide in which the surface-accessible residues have been altered; Cbx, carbenoxolone; Cx, connexin; Cyt*C*, cytochrome *C*; $[Ca^{2+}]_i$, cytoplasmic Ca^{2+} concentration; DAPI, 2′,6′-diamidino-2-phenylindole; DMEM, Dulbecco's modified Eagle's medium; DTR, dextran Texas Red; ER, endoplasmic reticulum; EV, empty vector; GJ, gap junction channel; HBSS-Hepes, Hanks' balanced salt solution buffered with Hepes; IDP, IP_3R-derived peptide; IP_3, inositol 1,4,5-trisphosphate; IP_3R, inositol 1,4,5-trisphosphate receptor; NALC, *N*-acetyl L-cysteine; PBSD+, PBS supplemented with Ca^{2+} and Mg^{2+}; PFA, paraformaldehyde; PI, propidium iodide; PLC, phospholipase C; PTP, permeability transition pore; ROS, reactive oxygen species; SCR, scrambled version of BH4-Bcl-2; SLDT, scrape loading and dye transfer; WT, wild-type

Received 10.8.11; revised 07.10.11; accepted 25.10.11; Edited by RA Knight; published online 25.11.11

GJ permeability, a more suitable candidate.[8,18,19] Moreover, its ER IP_3 receptor (IP_3R) channel is modulated by pro- and anti-apoptotic proteins,[1,3,7,20,21] and the ensuing Ca^{2+} changes may trigger Cyt*C* release from the mitochondria.[5]

Here, we examined the role of IP_3 in the communication of apoptosis from dying cells to surrounding healthy cells *via* GJs. Although this molecule is suggested to contribute to GJ-mediated spread of apoptosis,[13] it remains unsolved whether IP_3 diffusion *via* GJs is necessary and sufficient to provoke cell death in cells coupled by GJs. In this study, we aimed (i) to specifically interfere with IP_3 generation in the cells in which apoptosis was induced (trigger cells) and also in recipient cells receiving the cell death message *via* GJs, (ii) to interfere with the IP_3R in trigger and recipient cells and (iii) to interfere with the passage of IP_3 *via* GJs. Our results show that the cell death spreading process crucially relies on not only the GJ-mediated transfer of IP_3 but also requires other factors to convert this physiological messenger into an intercellular master in crime.

Results

Interfering with IP_3 signaling reduces the propagation of Cyt*C*-triggered apoptosis. We loaded a small and defined zone of cells within confluent rat C6-glioma cultures, stably transfected with Cx43 (C6Cx43), with 100 μM Cyt*C* to induce apoptosis (trigger zone) combined with 100 μM Dextran Texas Red (DTR) to identify the cells receiving the apoptotic trigger. Cell loading with these membrane-impermeable substances was performed by *in situ* electroporation that was optimized to avoid inducing cell death by itself.[11] After 6 h, significant apoptosis was detected in a 200 μm wide zone adjacent to the trigger zone (communication zone; Figure 1a). We previously demonstrated that GJs predominantly mediate the communication of apoptosis to this area.[11] To assess whether the Ca^{2+}-mobilizing messenger IP_3 and its ER-located receptor contribute to this process, we loaded membrane- and GJ-impermeable compounds that interfere with IP_3 signaling in the trigger or communication zone by *in situ* electroporation, and investigated their effect on cell death spread by quantifying apoptosis in the communication zone (Figure 1). As the agents applied are membrane and GJ impermeable, their action was limited to the loaded cell zone.

In a first set of experiments, we promoted IP_3 degradation by loading the cells in the trigger or communication zone with a human type I IP_3 5-phosphatase (MW 43 kDa), which specifically hydrolyses the phosphate group on the fifth position of the inositol moiety. Two controls were applied, one containing no enzyme and one with inactivated enzyme. We first checked the activity of these substances by monitoring their effect on changes in cytoplasmic Ca^{2+} concentration ($[Ca^{2+}]_i$) triggered by photolytic release of IP_3 from a caged inactive precursor (caged IP_3). We found that the active IP_3 5-phosphatase (loaded together with caged IP_3 in the same region) significantly suppressed the $[Ca^{2+}]_i$ changes, while the inactive enzyme had no effect (Figures 2a-c). To study its impact on the dissemination of Cyt*C*-induced cell death, we loaded the IP_3 5-phosphatase in the trigger zone, together with Cyt*C*. The spread of apoptosis, studied 6 h later in the communication zone, was significantly reduced in the presence of the active IP_3 5-phosphatase ($\sim$47% reduction) (Figure 2d). It is possible that the reduced occurrence of apoptosis in the communication zone results from a less potent stimulation of cell death in the trigger zone. However, the enzyme did not interfere with apoptosis generation induced by a lower concentration of Cyt*C* (10 μM, cell death quantified 25 min later) in this area (Figure 2e). Thus, the reduced cell death in the communication zone is not the outcome of reduced cell death in this area as such. Loading the IP_3 5-phosphatase in the communication zone instead of the trigger zone caused a significant reduction ($\sim$54%) of caspase-positive cells in the communication zone (Figure 2f). Collectively, these experiments demonstrate that enhancing IP_3 degradation in the trigger or communication zone reduces communication of apoptotic cell death.

In a second set of experiments, we investigated the role of the IP_3R in the propagation of cell death. Since currently available IP_3R inhibitors like xestospongin B/C or 2-aminoethoxydiphenyl borate are membrane-permeable substances, these compounds cannot be specifically targeted to either trigger or communication zone. Therefore, we exploited the BH4 domain of Bcl-2 (BH4-Bcl-2; MW 3.6 kDa) to suppress IP_3R channel opening. Bcl-2 is an anti-apoptotic member of the Bcl-2 family of proteins, which regulate the intrinsic pathway of apoptosis. It differs from the pro-apoptotic members by the presence of a BH4 domain, which is essential for its anti-apoptotic function.[22] In addition, the BH4 domain of Bcl-2 interacts with the IP_3R, thereby suppressing IP_3R-mediated Ca^{2+} release and preventing pro-apoptotic Ca^{2+} signaling.[23,24] We applied the following synthetic peptides (20 μM final concentration): BH4-Bcl-2 peptide (amino acids 6–30 of Bcl-2), a mutant BH4-Bcl-2 peptide in which the surface-accessible residues have been altered (BIND), a scrambled BH4-Bcl-2 (SCR) and an IP_3R-derived peptide (IDP) corresponding to the Bcl-2-binding site on the IP_3R (amino acids 1389–1408).[24] The latter acts as a sink for BH4-Bcl-2, selectively preventing its action on the IP_3R.[23] We first checked the outcome of these peptides on caged IP_3-induced $[Ca^{2+}]_i$ elevations (Figure 3a). BH4-Bcl-2 peptide suppressed the Ca^{2+} responses and IDP counteracted this effect, demonstrating that BH4-Bcl-2 inhibits IP_3R-mediated Ca^{2+} signaling by directly acting on the IP_3R. Next, we assessed their effect on the communication of apoptosis. Loading of the trigger zone with BH4-Bcl-2 (together with Cyt*C*) resulted in a significantly reduced percentage of caspase-positive cells in the communication zone ($\sim$47% reduction), whereas the control peptides (BIND, SCR) had no effect (Figure 3b). Most notably, the reduction of apoptosis by BH4-Bcl-2 was prevented by inclusion of IDP. The presence of BH4-Bcl-2 in the trigger zone did, however, significantly reduce cell death in this zone (tested with 10 μM Cyt*C*, cell death quantified 25 min later; Figure 3c). In conclusion, the cell death reduction in the communication zone may result from a combination of IP_3R inhibition and decreased cell death in the trigger zone with less production of cell death messengers. When BH4-Bcl-2 loading was performed in the communication zone, apoptosis was strongly suppressed in this zone ($\sim$65%) (Figure 3d). Thus, BH4-Bcl-2 too inhibits the deleterious action of IP_3 in the communication zone.

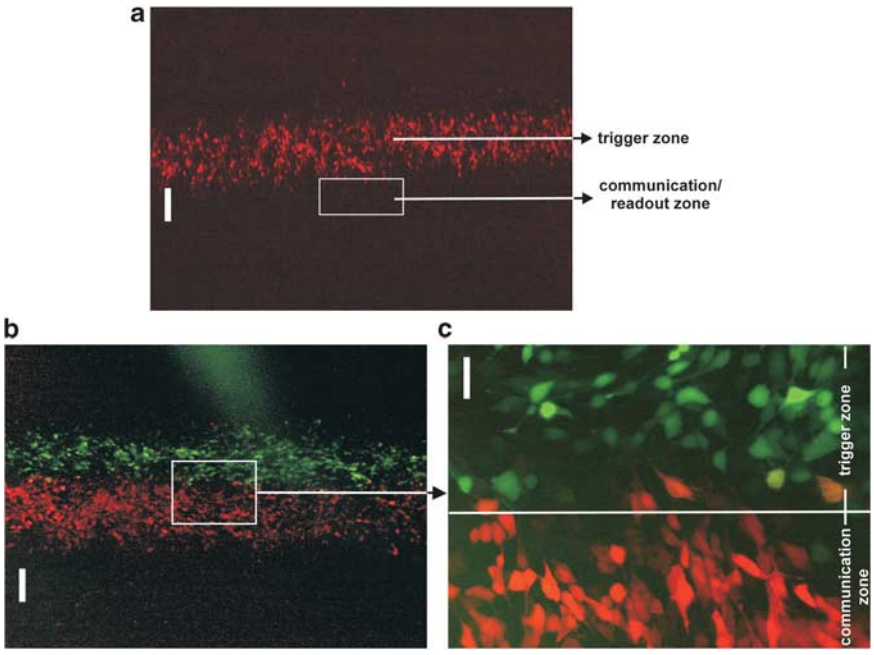

Figure 1 Analysis of propagation of Cyt*C*-induced apoptotic cell death in a remote non-Cyt*C*-loaded zone. (**a**) A small strip of cells of a C6Cx43 culture loaded with Cyt*C* together with DTR ('trigger zone' represented by the red staining) using the *in situ* electroporation technique. After 6 h, a caspase staining was performed and images were taken with a $\times 10$ objective in a region right next to the trigger zone.[11] The readout and quantification of bystander death was performed in a zone located 0–200 μm away from the trigger zone ('communication zone' indicated by the white rectangle). (**b** and **c**) Example of a dual electroporation. A C6Cx43 culture was loaded first with the human type I IP_3 5-phosphatase or IP_3R inhibitor BH4-Bcl-2 together with DTR in the communication zone. Subsequently, the trigger zone was loaded with Cyt*C* together with FITC-dextran. Apoptotic cell death was investigated 6 h after Cyt*C* loading in the communication zone. Note that (i) optimized settings resulted in practically no overlap between the two zones, and (ii) these images were taken immediately after electroporation. The scale bar measures 200 μm (**a** and **b**) and 50 μm (**c**)

Spread of Cyt*C*-induced cell death in a cell line containing GJs with an impaired permeability to IP_3. To obtain more information on whether IP_3 diffuses through GJs during Cyt*C*-induced cell death, we used a mutant Cx26 (Cx26V84L), which accounts for non-syndromic hearing loss.[25,26] Moreover, it forms GJs with a reduced permeability to IP_3.[26] For this purpose, rat C6-glioma cells were lentivirally transduced with cDNA encoding either human wild-type (WT) Cx26 or Cx26V84L. Cells transduced with the empty vector (C6EV) were used as a control. Western blot analysis demonstrated the presence of Cx26 in C6Cx26 and C6Cx26V84L, while no detectable Cx26 immunoreactivity was observed in C6EV (Figure 4a). These results were confirmed by immunostaining, which localized the expression of Cx26 in the cytoplasm as well as in the plasma membrane at regions of contact between adjacent cells (Figure 4b). GJ coupling was studied using the dyes calcein (622 Da, -4) and propidium iodide (PI) (414 Da, $+2$) (Figure 4c). Dye transfer was comparable between C6Cx26 and C6Cx26V84L, and significantly higher compared to the C6EV. Pre-incubation of C6Cx26 and C6Cx26V84L for 15 min with the GJ blocker carbenoxolone (Cbx; 50 μM) strongly limited coupling to levels similar to those observed in C6EV. Next, we analyzed the permeability of channels formed by Cx26V84L to IP_3 by monitoring intercellular Ca^{2+} wave propagation in response to photolytic release of IP_3 and in the presence of 10 U/ml of apyrase VI and VII. These ATP-degrading enzymes were included to abolish paracrine purinergic communication of Ca^{2+} wave propagation, leaving GJs as the only pathway for IP_3 diffusion.[27] After photolytically releasing IP_3 in cells located in the center of the field, $[Ca^{2+}]_i$ rapidly increased, and propagated to neighboring cells (Figure 4d). The extent of the Ca^{2+} wave was significantly reduced in C6Cx26V84L cells compared with C6Cx26. These results confirm that Cx26V84L GJs exhibit a reduced permeability to IP_3, while retaining the ability to transfer different tracers.[25,26] We then loaded the cell lines with Cyt*C* and determined the propagation of apoptosis. In C6Cx26, this procedure evoked cell death in the trigger zone followed by cell death spread to the communication zone, quantified 6 h later, as observed in C6Cx43 (Figure 4e). Cbx (50 μM), applied 15 min before Cyt*C* loading and maintained in the culture medium thereafter (15 min + 6 h), reduced apoptosis in the communication zone. Importantly, in C6Cx26V84L cells, apoptosis in the communication zone was reduced to the level observed in C6EV (Figure 4e). Furthermore, loading the IP_3 5-phosphatase in the trigger zone (together with Cyt*C*) significantly reduced apoptosis in the communication zone (Figure 4f). Loading of the IP_3 5-phosphatase in the communication zone also strongly suppressed apoptosis in the same area (Figure 4g).

IP_3 does not evoke cell death by itself. The previous experiments demonstrate that the diffusion of IP_3 through GJs is necessary for the communication of apoptosis. Hence, one may anticipate that IP_3 is sufficient as a messenger and that elevating IP_3 levels in the cells may ensue in cell death. However, loading the trigger zone of C6Cx43 cells with 50 μM IP_3 (by *in situ* electroporation, as for Cyt*C*) did not result in apoptosis, neither in the trigger zone ($1.38 \pm 0.3\%$ for IP_3 + DTR compared to $0.73 \pm 0.1\%$ for DTR-only; $n = 5$–6)

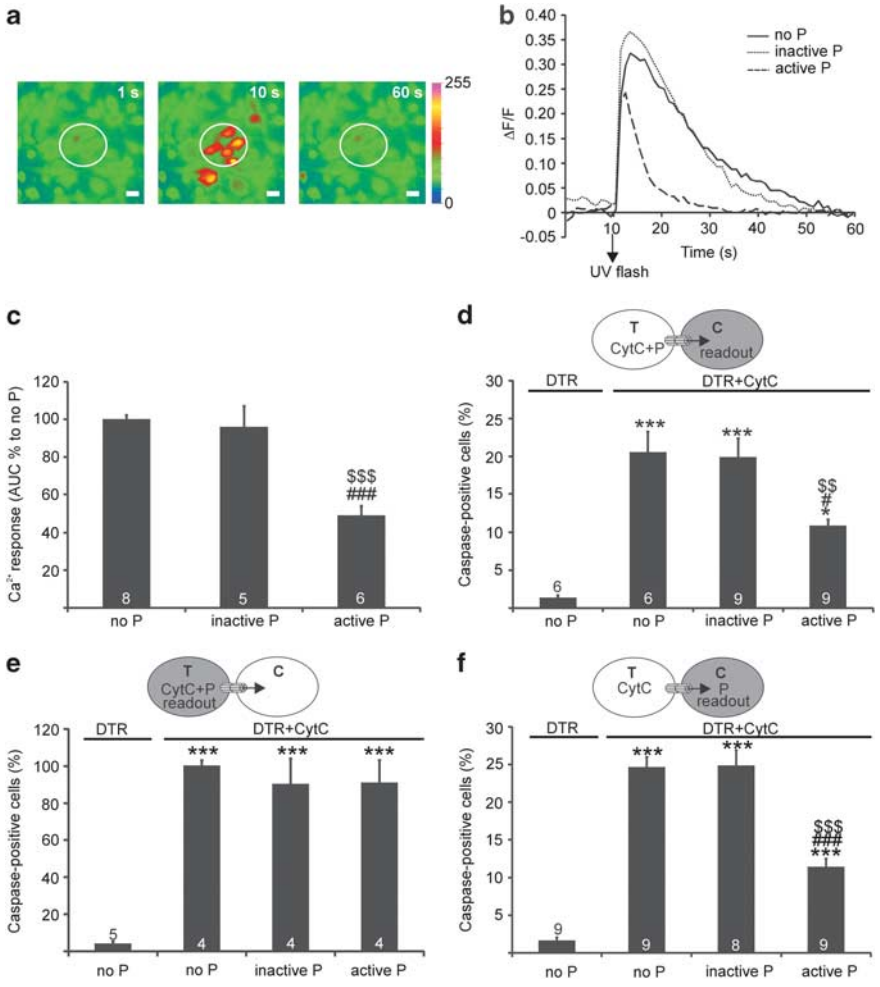

Figure 2 Degrading IP_3 by loading the cells with IP_3 5-phosphatase reduces the spread of apoptosis. (**a**) Representative images showing increases in $[Ca^{2+}]_i$ after photoliberation of caged IP_3 at 9980 ms of recording. The white circle depicts the area of uncaging and subsequent analysis. The scale bar measures 20 μm. (**b**) Traces of individual cells located in the uncaging area containing no IP_3 5-phosphatase (no P), the inactive compound (inactive P) or the active IP_3 5-phosphatase (active P). The AUC was quantified from these traces for each cell present in the uncaging area and is depicted in the next panel. (**c**) The active IP_3 5-phosphatase significantly reduced caged IP_3-induced Ca^{2+} responses, while the inactive compound had no effect. The conditions with inactive and active IP_3 5-phosphatase were normalized to the condition without IP_3 5-phosphatase. (**d**) The active IP_3 5-phosphatase significantly decreased apoptosis in the communication zone 6 h after loading the enzyme together with Cyt*C* in the trigger zone. (**e**) The active IP_3 5-phosphatase had no influence on apoptosis induction in the trigger zone, measured 25 min after loading the enzyme together with Cyt*C* in this area. The conditions with inactive and active IP_3 5-phosphatase were normalized to the condition without IP_3 5-phosphatase. (**f**) The active IP_3 5-phosphatase significantly reduced the propagation of cell death 6 h after loading in the communication zone. Illustrations above the bar chart in panels **d–f** indicate where Cyt*C* and the IP_3 5-phosphatase were loaded and where apoptosis was quantified (grey cell-readout). Graphs represent mean ± S.E.M.; numbers on the bars indicate '*n*'; *significance compared to loading with DTR-only; #significance compared to the corresponding bar of the control without IP_3 5-phosphatase; and $significance compared to the corresponding bar of the inactive enzyme. One symbol indicates $P<0.05$, two symbols indicate $P<0.01$ and three symbols indicate $P<0.001$ (P, IP_3 5-phosphatase; C, communication zone; T, trigger zone)

nor in the communication zone (Figure 5a). Even very high concentrations, up to 200 μM, were ineffective. However, combining IP_3 loading in the trigger zone with a low concentration of Cyt*C* (10 μM) potentiated apoptosis in the communication zone, compared to loading with Cyt*C* alone (Figure 5a). These results are indicative of a cooperative action of IP_3 with other messengers released upon cell death. A plausible co-candidate is Ca^{2+}, which is importantly intertwined in the cascade leading to apoptosis, including the signaling cascade activated by Cyt*C*.[11,13,16] To determine whether Ca^{2+} acts in cooperation with IP_3, we loaded the cells with 50 μM IP_3 in the presence of a subtoxic concentration (2 μM) of the Ca^{2+} ionophore A23187 (applied immediately after IP_3 loading and present the next 6 h) to induce a $[Ca^{2+}]_i$ elevation. Similar to IP_3 loading without associated $[Ca^{2+}]_i$ elevation, no apoptosis was observed 6 h later in the trigger zone ($0.81 \pm 0.2\%$ for $IP_3 +$ A23187 compared to $1.29 \pm 0.2\%$ for IP_3 and $0.85 \pm 0.1\%$ for A23187; $n = 4$) and communication zone (Figure 5b). To test whether ER-derived Ca^{2+}, instead of extracellular-derived Ca^{2+}, is more potent, we repeated this experiment with a subtoxic concentration of the SERCA pump inhibitor thapsigargin (2.5 μM), a treatment that causes ER emptying by Ca^{2+} leakage from the store and accelerates staurosporine-induced apoptosis.[28] With thapsigargin in the culture medium, IP_3 (50 μM) loading of the trigger zone induced a small but significant increase of caspase-positive cells 6 h later in this zone ($4.77 \pm 2.7\%$ for $IP_3 +$ thapsigargin compared to $1.29 \pm 0.2\%$ for IP_3 and

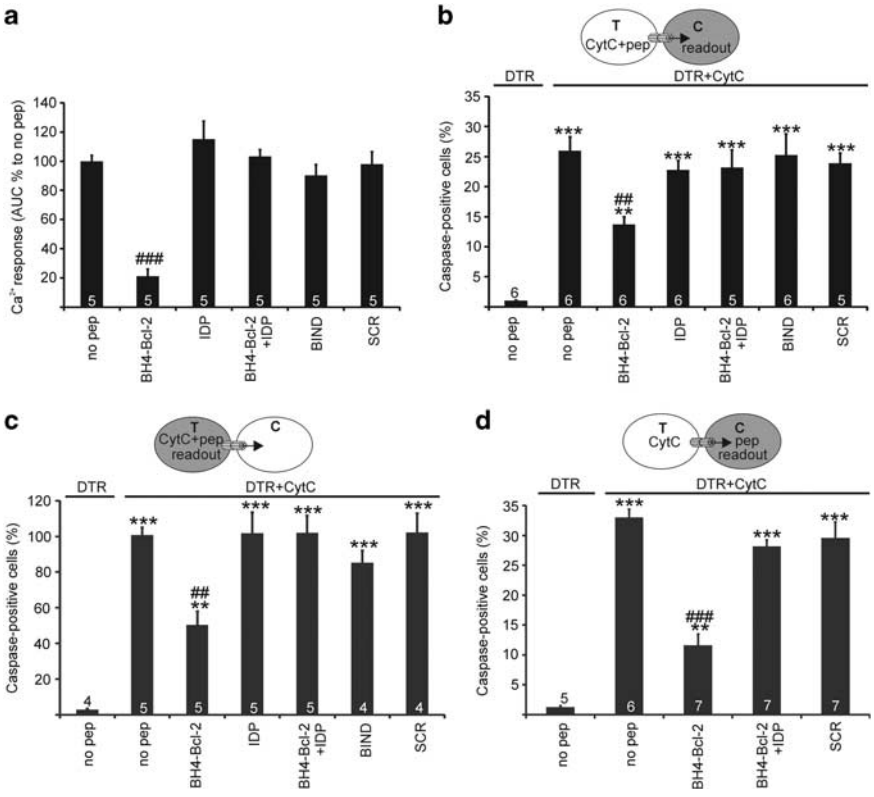

Figure 3 Inhibiting the IP_3R by loading the cells with the BH4-Bcl-2 peptide reduces the spread of apoptosis. (**a**) The BH4-Bcl-2 peptide significantly reduced caged IP_3-induced Ca^{2+} responses, while the set of control peptides (SCR and BIND) and a combination of BH4-Bcl-2 and IDP had no effect. The conditions with peptides were normalized to the condition without peptides. (**b**) BH4-Bcl-2 significantly decreased apoptosis in the communication zone 6 h after loading the peptide together with Cyt*C* in the trigger zone. The control peptides or BH4-Bcl-2 + IDP had no significant effect. (**c**) BH4-Bcl-2 significantly reduced apoptosis in the trigger zone 25 min after loading the peptide together with Cyt*C* in the trigger zone. The different conditions were normalized to the condition without peptide. (**d**) BH4-Bcl-2 significantly reduced cell death propagation 6 h after loading in the communication zone. Illustrations above the bar chart in panels **b–d** indicate where Cyt*C* and the peptides were loaded and where apoptosis was quantified (grey cell-readout). Graphs represent mean ± S.E.M.; numbers on the bars indicate '*n*'; *significance compared to loading with DTR-only; and #significance compared to the corresponding bar of the control without peptide. One symbol indicates $P<0.05$, two symbols indicate $P<0.01$ and three symbols indicate $P<0.001$ (pep, peptide; C, communication zone; T, trigger zone)

1.29 ± 0.3% for thapsigargin; $n=4$; $P<0.05$) and in the communication zone (Figure 5b).

Mitochondrial Ca^{2+} overload can lead to apoptosis through generation of reactive oxygen species (ROS).[29] ROS may be transferred *via* GJs, can modulate Ca^{2+} dynamics and augment the Ca^{2+} surge.[29,30] We examined whether ROS cooperates with IP_3 to evoke cell death. Measurement of ROS production with CM-H_2DCFDA demonstrated a gradual increase of the fluorescence signal over the 6 h period after Cyt*C* loading (Figure 5c). This increase was blocked by the antioxidant *N*-acetyl L-cysteine (NALC) (1 mM) applied in the medium (added 30 min before Cyt*C* loading and present 6 h thereafter). Such treatment did, however, not influence cell death 6 h later in the communication zone (Figure 5d).

Discussion

The present work demonstrates that the communication of Cyt*C*-induced apoptosis critically relies on (i) the presence of IP_3 in both the apoptosis trigger zone and cell death communication zone, and (ii) the presence of GJs permeable to IP_3 (Figure 6 and Table 1).

Studies conducted over the past 20 years indicated a crucial role for GJs in the communication of cell death.[10] One major caveat in this research area still relates to identifying the signals that convey the cell death message. A previous study has already provided important insights, that is, that a minimal gap junctional conductance is necessary to obtain apoptosis in a neighbor coupled cell and that IP_3 (based on work with the IP_3R inhibitor xestospongin C) is a strong candidate for passing the death message via GJs.[13] To unveil the role of IP_3 and its receptor in our experimental setting, we applied various tools interfering with IP_3-mediated Ca^{2+} signaling: an IP_3 5-phosphatase,[31,32] and the BH4 domain of Bcl-2 as an IP_3R blocker.[23,24] *In situ* electroporation allows loading spatially defined trigger or communication zones with these high-molecular-weight cell-impermeable agents that become trapped in the cells upon introduction. The observed reduction of the spread of cell death after application of IP_3 5-phosphatase or BH4-Bcl-2 in the trigger or communication zone implies that (i) the generation of IP_3 in trigger zone and (ii) the presence of IP_3 in the communication are both necessary events for cell death propagation to occur. There is general agreement that a tight interplay between the ER and mitochondria is a control point for apoptosis.[4] More specifically,

a strategic positioning of the sites of IP_3R-mediated Ca^{2+} release in close proximity of the mitochondria results in the formation of an 'ER-to-mitochondria conduit', mitochondrial Ca^{2+} overload, permeability transition pore (PTP) opening and subsequent release of pro-apoptotic molecules including CytC.[3,5] A recent report demonstrates that microinjection of IP_3 in astrocytes can also evoke Bax translocation to mitochondrial membranes and is accompanied by Ca^{2+}

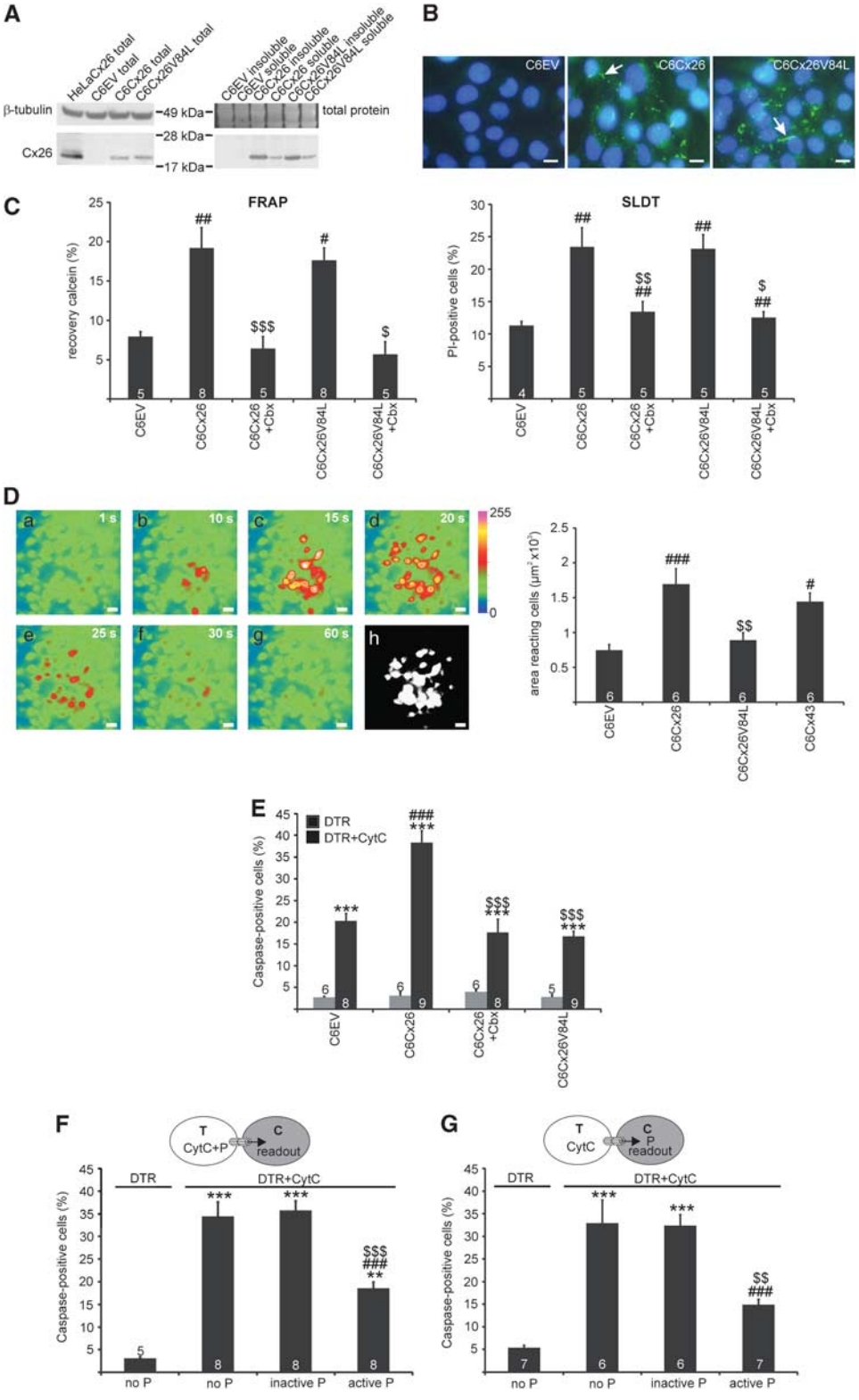

wave propagation to neighboring cells.[33] In turn, an elevation of $[Ca^{2+}]_i$ may provide a positive feedback mechanism for phospholipase C (PLC) activation to generate IP_3.[19]

Several regulatory mechanisms exist that influence the IP_3R activity and enable them to modulate Ca^{2+}-dependent apoptotic pathways.[3] Our finding that BH4-Bcl-2, by inhibiting the IP_3R, significantly reduced Cyt*C*-induced apoptosis confirms the previously identified feedforward mechanism. This vicious circle consists of an interaction of Cyt*C* with the IP_3R and alleviation of the inhibitory effect of high $[Ca^{2+}]_i$ on the IP_3R, thereby promoting Ca^{2+} release from the ER and accumulation into the mitochondria with more Cyt*C* release and caspase activation as a consequence.[1,24] Thus, the presence of the IP_3R is a prerequisite for the development of Cyt*C*-induced apoptosis, which seems to be in contrast to the IP_3 molecule itself. In our experimental model, the IP_3 5-phosphatase had no discernible effect on cell death in the trigger zone. However, it has to be noted that (i) an incomplete

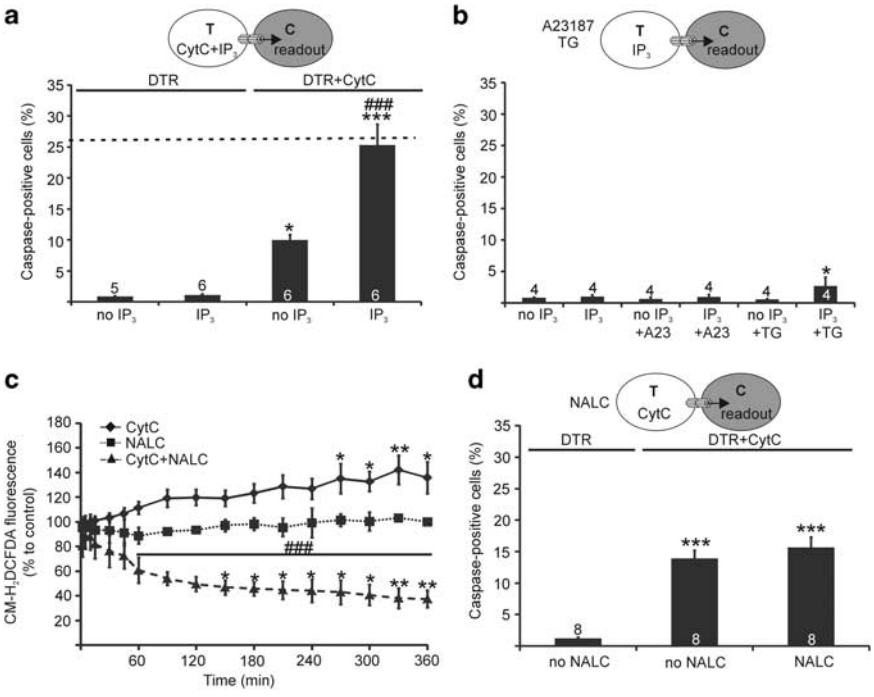

Figure 5 IP_3 alone or combined with Ca^{2+} is not sufficient to evoke cell death spread. (**a**) Loading C6Cx43 cells with IP_3 did not result in apoptosis in the communication zone 6 h after loading. However, combining IP_3 with 10 μM Cyt*C* in the trigger zone potentiated cell death in the communication zone 6 h later. The percentage of caspase-positive cells in the communication zone was comparable to the AI after electroporation of 100 μM Cyt*C* without IP_3 (dashed line). (**b**) IP_3 loading combined with A23187 treatment did not evoke cell death dissemination, while the application of thapsigargin (TG) caused a slight increase of apoptosis in the communication zone 6 h later. (**c**) Cyt*C* loading resulted in a gradual increase in ROS as measured by an augmentation of the fluorescence of CM-H_2DCFDA. NALC, applied 30 min before and during 6 h after Cyt*C* loading, blocked the production of ROS. The different conditions were normalized to the condition without Cyt*C* and NALC ($n = 5$–9). (**d**) Exposing the cells in the trigger and communication zone to NALC had no influence on spread of apoptosis to the communication zone. Illustrations above the bar chart in panels **a**, **b** and **d** indicate where Cyt*C*, IP_3, A23187, thapsigargin and NALC were applied and where apoptosis was quantified (grey cell-readout). Graphs represent mean ± S.E.M.; numbers on the bars indicate '*n*'; *significance compared to cultures loaded with IP_3 (**a** and **b**), loading with DTR-only without NALC (**c** and **d**); #significance compared to the corresponding bar of the culture loaded with Cyt*C* but no IP_3 (**a**) or Cyt*C* (**c**). One symbol indicates $P < 0.05$, two symbols indicate $P < 0.01$ and three symbols indicate $P < 0.001$ (TG, thapsigargin)

Figure 4 GJs with impaired permeability to IP_3 reduce the spread of apoptosis. (**A**) Western blot analysis for Cx26 in the transduced cell lines C6EV, C6Cx26 and C6Cx26V84L. Cx26 expression in total protein lysates and after separation of the Triton X-100 soluble and insoluble fractions; the latter representing the fraction incorporated into GJs. Cx26 expression was comparable between C6Cx26 and C6Cx26V84L, but was absent in C6EV. HeLaCx26 was used as a positive control. β-Tubulin or total protein staining report equal loading. (**B**) Overlays of a Cx26 immunostaining (green) and nuclear DAPI staining (blue). The Cx26 expression pattern was similar for Cx26WT and its mutant form, with arrows indicating the presence of gap junctional plaques. The scale bar measures 20 μm. (**C**) Gap junctional coupling in the different cell lines as studied with fluorescence recovery after photobleaching (FRAP) and SLDT. Gap junctional coupling was comparable for C6Cx26 and C6Cx26V84L and was inhibited by application of Cbx. (**D**) Example images showing the dissemination of a Ca^{2+} wave in C6Cx26 after photoliberation of caged IP_3 at 9980 ms and in the presence of the ATP-degrading enzyme apyrase (a–g). Images recorded during 60 s were corrected for cells reacting immediately to the UV flash, subjected to a threshold and averaged (h). The area of reacting cells was quantified from this image and is depicted in the graph. The V84L mutation significantly reduced caged IP_3-induced Ca^{2+} waves. The scale bar measures 20 μm. (**E**) Spread of Cyt*C*-induced apoptosis to the communication zone in the different cell lines measured 6 h after loading. A significantly smaller percentage of caspase-positive cells were detected in the communication zone of C6EV and C6Cx26V84L compared to C6Cx26. Cbx reduced the propagation of apoptosis in C6Cx26 to the level of C6EV. (**F**) The active IP_3 5-phosphatase significantly decreased apoptosis in the communication zone of C6Cx26 cultures 6 h after loading the enzyme together with Cyt*C* in the trigger zone. (**G**) The active IP_3 5-phosphatase also significantly reduced the spread of cell death 6 h after loading in the communication zone. Illustrations above the bar chart in panels **F** and **G** indicate where Cyt*C* and the IP_3 5-phosphatase were loaded and where apoptosis was quantified (grey cell-readout). Graphs represent mean ± S.E.M.; numbers on the bars indicate '*n*'; *significance compared to loading with DTR-only (**E–G**); #significance compared to the corresponding bar of C6EV (**C–E**) or the corresponding control without phosphatase (**F** and **G**); $significance compared to C6Cx26 (**C–E**) or the inactive phosphatase (**F** and **G**). One symbol indicates $P < 0.05$, two symbols indicate $P < 0.01$ and three symbols indicate $P < 0.001$ (P, IP_3 5-phosphatase; C, communication zone; T, trigger zone)

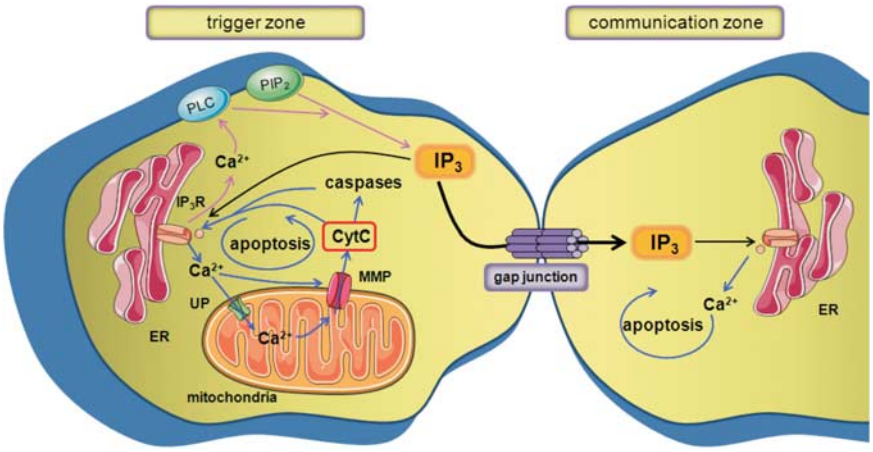

Figure 6 Scheme sketching a hypothetical model for the involvement of IP_3 in the propagation of Cyt*C*-induced apoptosis. After introduction of Cyt*C* in the trigger zone, the pro-apoptotic molecule interacts with the IP_3R, resulting in the abolishment of the Ca^{2+}-dependent inhibition of the IP_3R. Consequently, a vicious circle is activated (depicted in blue), consisting of ER Ca^{2+} release, mitochondrial Ca^{2+} accumulation, Cyt*C* release and caspase activation. Furthermore, IP_3-induced Ca^{2+} release from the ER can provide a positive feedback mechanism for PLC activation and subsequent IP_3 generation (depicted in pink). A small amount of IP_3 is transferred through GJs and results in apoptosis in the cells in the communication zone. However, additional messengers or conditions seem to be required to convert IP_3 into a pro-apoptotic molecule. The figure was produced using Servier Medical Art (MMP, mitochondrial membrane permeabilization; UP, uniporter)

Table 1 Summary of the effects of the different substances on apoptosis in the trigger and/or communication zone

Compound	Loading zone	Readout zone	Effect on apoptosis
Cyt*C*	T	T	X
		C	−
+IP_3 5-phosphatase	C	C	−
Cyt*C*	T	T	−
		C	−
+BH4-Bcl-2	C	C	−
IP_3	T	T	X
		C	X
+Cyt*C*	T	C	+
+A23187	T+C	T	X
		C	X
+thapsigargin	T+C	T	+
		C	+
NALC	T+C	C	X

Abbreviations: X, no effect; −, decrease of apoptotic cells in the readout zone; +, increase in apoptotic cells in the readout zone; T, trigger zone; C, communication zone

degradation of IP_3 was observed after flash photolysis of caged IP_3, (ii) a small amount of IP_3 might be sufficient to spark the vicious cell death cycle and (iii) the IP_3R can be activated indirectly through the proteolysis by caspase 3, providing a continuous Ca^{2+} leak from the ER.[20,21]

Peixoto *et al*.[34] recently demonstrated that Bax and/or Bak are required to mediate bystander death induced by transfection of a plasmid encoding GFP-Bax in Bax and Bak double-knockout mouse embryonic fibroblasts. Many intrinsic apoptotic signals seem to rely on both the release of Ca^{2+} from the ER and the presence of Bax and Bak to execute apoptosis.[33,35] It is important to note that these pro-apoptotic Bcl-2 family members not only act at the level of the mitochondria, but also at the ER. Bax has been demonstrated to promote caspase-independent Ca^{2+} mobilization from the ER to the mitochondrion through the uniporter during apoptosis,[28] and to promote Ca^{2+} wave propagation to neighboring cells.[36] On the other hand, reduced ER Ca^{2+} levels and a decreased mitochondrial Ca^{2+} uptake were observed in the Bax- and Bak-deleted mouse embryonic fibroblasts. In this case, increased binding of Bcl-2 to IP_3R1 caused IP_3R sensitization, resulting in a basal IP_3R-mediated Ca^{2+} leak, thereby decreasing the sensitivity to apoptotic Ca^{2+} signaling.[35,37] Of note, in our model, the BH4-Bcl-2 peptide also interacts with the IP_3R and inhibits IP_3-induced Ca^{2+} signaling, but does not influence steady-state ER Ca^{2+} levels as reported recently.[24] Although distinct actions of pro- *versus* anti-apoptotic Bcl-2 members in controlling Ca^{2+} dynamics have been demonstrated, they could both regulate bystander death via a direct or indirect modulation of IP_3-induced Ca^{2+} release.

Convincing evidence to substantiate a role for IP_3 as the cell death messenger passing through GJs was obtained in the Cx26V84L cells. While the V84L mutation is characterized by a proper intracellular sorting and similar gap junctional conductances as the Cx26WT,[26] Cx26V84L-based GJs displayed significantly impaired permeation to IP_3 as observed in the spread of intercellular Ca^{2+} waves.[26] Several lines of evidence point to IP_3 as the responsible messenger for

Ca^{2+} wave propagation via GJs composed of Cx26, Cx43 or Cx32.[8,38] Hence, the reduced spread of apoptosis in C6Cx26V84L cells is related to the defective gap junctional diffusion of IP_3. Importantly, the dissemination of cell death in the C6Cx26 experiments was similar to that in C6Cx43 cells (1.89 ± 0.14-fold more for C6Cx26/C6EV and 1.64 ± 0.078-fold more for C6Cx43/C6WT) and the size of the intercellular Ca^{2+} waves did not differ either.

Additional experiments indicated that Ca^{2+} signals produced by IP_3 are handled normally, but potentiated apoptosis spread when superimposed with a low concentration of Cyt*C*. Accordingly, Szalai *et al*.[5] demonstrated that IP_3Rs release very small amounts of Ca^{2+} to evoke transient PTP opening, mitochondrial depolarization and apoptosis in cells primed with a subtoxic apoptotic trigger. However, under physiological conditions, the event of PTP opening was relatively insensitive to IP_3-induced Ca^{2+} signals.[5] The mitochondria have been proposed to function as 'coincidence detectors' as oxidative stress-induced apoptosis requires a synergism between high mitochondrial Ca^{2+} and ROS production to open the PTP and activate caspases.[39] Combining IP_3 with exposure to thapsigargin resulted in a small but significant increase in apoptosis spread in our model system, likely by potentiating mitochondrial Ca^{2+} overload. In addition, the interplay between Ca^{2+} dynamics and IP_3 metabolism may also play a role. Fluctuations in $[Ca^{2+}]_i$ do not only influence IP_3 production but also its degradation. Binding of Ca^{2+}/calmodulin to the IP_3 3-kinase enhances its activity, thereby modulating IP_3 levels and increasing the concentration of inositol 1,3,4,5-tetrakisphosphate. The latter has a 30 times larger half-life than IP_3, may act to sustain Ca^{2+} signals initiated by IP_3 and thus contribute to its pathological function.[40] Whether the apoptotic signaling pathway in the communication zone proceeds through the above-mentioned vicious circle has to be further investigated. Preliminary experiments with a peptide reported to disrupt the interaction between the IP_3R and Cyt*C*, and to inhibit both extrinsic and intrinsic apoptosis,[1] counteracted caspase activation in the trigger[24] and communication zone (unpublished observation). These results corroborate the view of a central role for Cyt*C*/IP_3R signaling in triggering cell death in both areas.

We conclude from this work that the production of IP_3 in apoptotic cells, its diffusion through GJs and its actions in recipient cells are important for spreading apoptosis to neighboring cells. IP_3 is the key necessary messenger in this process, but other factors seem to be necessary to create conditions in which IP_3 will exert pro-apoptotic effects.

Materials and Methods

Agents. A23187, (caged) IP_3, calcein-AM, CM-H_2DCFDA, 10 kDa DTR, Fluo-3-AM, Hoechst 33342, PI and pluronic F-127 were purchased from Invitrogen (Merelbeke, Belgium). Apyrase (potato) grade VI and VII; Cbx, Cyt*C* from equine heart, 2′,6′-diamidino-2-phenylindole (DAPI), 10 kDa FITC-dextran, NALC, paraformaldehyde (PFA) and probenecid were obtained from Sigma (Bornem, Belgium). The synthetic BH4-domain peptides and IDP were derived from Thermo Electron (Karlsruhe, Germany).[24] Purification and determination of the activity of the human type I IP_3 5-phosphatase (6 μmol/min per ml) were performed as described previously.[32] The enzyme was used at a final dilution of 1/5000, which is based on previous experimental work with this compound,[31] taking into account an electroporation loading efficiency of $\sim$27%.[11] The IP_3 5-phosphatase was inactivated at 100 °C for 1 h.

Plasmid construction. The coding region of human Cx26WT and Cx26V84L were amplified by PCR from plasmids Cx26 pIRES-EGFP and Cx26V84L pIRES-EGFP,[26] using the following primers: forward, 5′-ATCCGGTACCGAATTCACCAT GGATTGGGGCACGCTG-3′ and reverse, 5′-GTCTAGATATCTCGAGTTAAACTG GCTTTTTTGACTTC-3′. The PCR products were cloned in pENTR3C vectors (Invitrogen) using In-Fusion cloning reaction (Takara Bio Europe/Clontech, Saint-Germain-en-Laye, France) according to the manufacturer's instructions. Subsequently, genes encoding Cx26WT and Cx26V84L were moved to bicistronic vectors to generate pdWPI-IRES-dsRed-Cx26WT and pdWPI-IRES-dsRed-Cx26V84L, respectively, through an LR recombination reaction (Clonasae Enzyme Mix; Invitrogen) according to the manufacturer's instructions. All constructs were sequenced at the VIB sequencing facility (ABI3730XL; Applied Biosystems, Carlsbad, CA, USA).

Cell culture. Rat C6-glioma cells were cultured in Dulbecco's modified Eagle's medium (DMEM) and Ham's F12 (1 : 1), containing 10% fetal bovine serum, 100 U/ml penicillin, 100 μg/ml streptomycin, 2.5 μg/ml fungizone and 2 mM glutamine (Gibco, Merelbeke, Belgium) at 37 °C, 5% CO_2.

Generation of lentivirus and transduction. HEK293T cells were grown in DMEM supplemented with 10% fetal calf serum (Gibco). HEK293T cells were seeded in 25 cm^2 flasks at 1.5×10^5 cells per ml and transfected the following day using the Ca^{2+} phosphate method with 4 μg of pdWPI-IRES-dsRed-Cx26WT or pdWPI-IRES-dsRed-Cx26V84L. Each transfection also included 1.2 μg of a plasmid encoding VSV-G (pMD2-VSV-G; Tronolab, Lausanne, France) and 2.6 μg of a plasmid encoding packaging proteins (pCMVdR8.9; Tronolab). VSV-G-pseudotyped virus was collected 24 h after transfection, passed through 0.45 μm filters and then added to the exponentially growing C6 cell cultures in the presence of 8 μg/ml of polybrene. Two sequential infections were carried out, each one for 24 h. The cells were expanded and then sorted on the EPICS ALTRA flow cytometer (Beckman Coulter, Analis SA, Suarlée, Belgium) for red-positive cells.

Electroporation loading. Cells were grown to near confluency on 4-well plates, 13 or 18 mm diameter glass coverslips depending on the ensuing experiment (oxidative stress measurements, apoptosis detection or caged IP_3 photoliberation). Cell monolayer cultures were washed three times with Hanks' balanced salt solution buffered with Hepes (HBSS-Hepes) supplemented with glucose (0.81 mM $MgSO_4 \cdot 7H_2O$, 0.95 mM $CaCl_2 \cdot 2H_2O$, 137 mM NaCl, 0.18 mM $Na_2HPO_4 \cdot 2H_2O$, 5.36 mM KCl, 0.44 mM KH_2PO_4, 5.55 mM D-glucose, 25 mM Hepes, pH 7.4) and subsequently three times with a low conductivity electroporation buffer (4.02 mM KH_2PO_4, 10.8 mM K_2HPO_4, 1.0 mM $MgCl_2$, 300 mM sorbitol, 2.0 mM Hepes, pH 7.4). They were placed 400 μm underneath a two-wire Pt-Ir electrode on the microscopic stage and electroporated in the presence of a tiny amount of electroporation solution (10 μl) containing 100 μM Cyt*C* and 100 μM 10 kDa DTR. Control cultures were electroporated with solution containing only 100 μM DTR. In some cases, where a restricted amount of apoptosis was required, lower Cyt*C* concentrations (10 μM) were applied (see Results section). Electroporation was carried out with 50 kHz bipolar pulses applied as trains of 10 pulses of 2 ms duration each and repeated 15 times. The field strength was 100 V peak-to-peak applied over a 500 μm electrode separation distance. After electroporation, cells were thoroughly washed with HBSS-Hepes.

In the dual electroporation protocol, two areas were subsequently loaded with different substances (Figures 1b and c). A first zone ('communication zone') was electroporated with substances interfering with the IP_3 signaling machinery (see Results section) together with 100 μM DTR. Subsequently, the culture was washed three times with HBSS-Hepes and three times with electroporation buffer after which it was placed again on the microscopic stage. The DTR electroporated zone was located using epifluorescence settings and positioned horizontally. The upper wire of the electrode was placed right underneath the red-stained area, 400 μm above the cells. A second zone ('trigger zone') was loaded with 100 μM Cyt*C* and 100 μM FITC-dextran. These settings resulted in practically no overlap between the two zones. Visual inspection of the fluorescent areas right after electroporation allowed one to evaluate the precise position of the two electroporated regions.

Apoptosis detection. After electroporation, cells were kept in 200 μl culture medium until scored for the apoptotic index (AI). This procedure consisted of detecting caspase-positive cells by staining with 10 μM of the CaspACE FITC-VAD-FMK *In situ* Marker from Promega (Promega Benelux, Leiden, The Netherlands) in HBSS-Hepes for 40 min at 37 °C. After fixing the cells with 4% PFA for 25 min at

room temperature, nuclei were additionally stained for 5 min with 1 μg/ml DAPI in PBS supplemented with Ca^{2+} and Mg^{2+} (PBSD+). Cells were mounted with Vectashield fluorescent mounting medium (VWR International, Leuven, Belgium) on glass slides. After staining, five images (in each culture) were taken in the zone adjacent to the Cyt*C* loaded zone containing the 'communication zone' (Figure 1a) using a Nikon TE300 epifluorescence microscope equipped with a $\times$10 objective (Plan APO, NA 0.45; Nikon) and a Nikon DS-Ri1 camera (Nikon Belux, Zaventem, Belgium). The number of caspase-positive cells were counted in each image and expressed relative to the number of nuclei present and stated as the AI. Small groups of apoptotic bodies were counted as remnants of a single apoptotic cell. Analyses were carried out blinded and making use of custom-developed counting software.

Caged IP_3 loading and photolytic release. Cells were seeded on 18 mm diameter glass coverslips and ester-loaded for 25 min with 5 μM Fluo-3-AM in HBSS-Hepes supplemented with 1 mM of probenecid and 0.01% pluronic F-127 at 37 °C, followed by a de-esterification over 15 min. Subsequently, cells were loaded with 50 μM caged IP_3 and 100 μM DTR using the *in situ* electroporation technique as described above. Imaging was carried out using an inverted fluorescence microscope equipped with an $\times$40 oil-immersion objective (S Fluor, NA 1.30; Nikon) and an intensified CCD camera (Extended Isis camera, Photonic Science, East Sussex, UK). A total of 60 images were generated at 1 image per s with the software written in Microsoft Visual C++ 6.0. After 10 s, IP_3 photolysis was induced by 20 ms spot illumination with a 1 kHz pulsed UV laser source (349 nm UV laser Explorer; Spectra-Physics, Newport, Irvine, CA, USA) (1800 μJ energy measured at the entrance of the microscope epifluorescence tube). Fluorescence intensity changes in cells in a region delineated by the UV laser beam width at 15% of its maximum energy were analyzed with custom-developed FluoFrames software (L Leybaert, Ghent, Belgium) (Figure 2a). Ca^{2+} changes were quantified as the area under the curve (AUC) of the separate Ca^{2+} traces (Figure 2b). A UV flash was applied at five different zones along the electroporated area per dish. For the Ca^{2+} wave experiments, cultures were loaded with 100 μM caged IP_3 and a UV flash was applied at at least 10 different places along the electroporated area per dish in the presence of 5 U/ml apyrase VI and VII. Images were calculated for relative fluorescence changes and an image taken right after the UV flash was subtracted to eliminate cells responding directly to the flash. The propagation of intercellular Ca^{2+} waves was expressed as the area of cells displaying fluorescence changes at least 5% above of the resting value.

Immunocytochemistry. Cells on coverslips were fixed for 25 min with 4% PFA and permeabilized for 10 min with 0.2% Triton X-100. Cells were immunolabeled overnight with polyclonal rabbit anti-Cx26 antibody (1/50 dilution in PBSD+ with 0.4% gelatin; Invitrogen) and subsequently incubated for another hour with secondary Alexa 488-conjugated goat anti-mouse IgG (1/500 dilution; Invitrogen). The nuclei were stained with 1 μg/ml DAPI in PBSD+ for 10 min and cells were mounted with Vectashield fluorescent mounting medium onto glass slides. All steps were carried out at room temperature and cell cultures were rinsed thoroughly with PBSD+ between all incubation steps. Samples were examined and photographed with the microscope as described for apoptosis detection using a $\times$40 oil-immersion objective.

Western blotting. Cells were seeded in 75 cm^2 falcons. Total cell protein lysates were extracted in ice-cold radio-immuno precipitation assay buffer and sonicated five times for 10 s. For separation of Triton X-100 soluble and insoluble fractions, cells were harvested in ice-cold 1% Triton X-100 in PBS supplemented with 50 mM NaF, 1 mM Na_3VO_4, 1% protease inhibitor cocktail (Sigma), 1% phosphatase inhibitor cocktail 1 and 2 (Sigma) and mini-EDTA-free protease cocktail (Roche Diagnostics, Penzberg, Germany). Samples were separated into a soluble and insoluble fraction by centrifugation at 16 000 $\times$ *g* for 10 min. Insoluble pellets were resuspended in Laemmli sample buffer and sonicated five times for 10 s. Protein concentrations were determined using a Bio-Rad DC protein assay kit (Bio-Rad, Nazareth, Belgium). Thereafter, 50 μg of protein lysates were separated on a 4–12% Bis–Tris gel (Invitrogen) and subsequently transferred onto a nitrocellulose membrane (Amersham Pharmacia Biotech, Buckinghamshire, UK). Membranes were blocked with 5% non-fat milk in Tris-buffered saline containing 0.1% Tween-20 and probed with the polyclonal rabbit anti-Cx26 antibody (1/2000 dilution; Invitrogen), followed by secondary alkaline phosphatase-conjugated goat anti-rabbit IgG antibody (1/8000 dilution; Sigma). Detection was carried out using the BCIP/NBT kit (Zymed, Invitrogen) according to the manufacturer's instructions. As a loading control, the membranes were immunoblotted for rabbit anti-β-tubulin antibody (1/1000; Abcam, Cambridge, UK), followed by a secondary horse radish peroxidase-conjugated anti-rabbit IgG antibody (1/1000 dilution; Cell signaling, Leiden, The Netherlands) and detected with Lumiglo chemiluminescent substrate (Cell signaling). Total protein staining was carried out with SYPRO Ruby protein blot dye (Invitrogen, Molecular Probes, Merelbeke, Belgium).

Fluorescence recovery after photobleaching. Cells were seeded on 9.2 cm^2 Petri dishes (TPP, Trasadingen, Switzerland) and experiments were carried out at near confluency. Cells were loaded for 40 min at room temperature with the GJ-permeable fluorescent tracer calcein-AM (10 μM) in HBSS-Hepes, followed by a de-esterification over 15 min. After extensive rinsing, cultures were transferred to the stage of a custom-made video-rate confocal laser scanning microscope. Fluorescence within a single cell was photobleached by a 1 s spot exposure to 488 nm Argon laser light and dye influx from neighboring cells was recorded over the next 5 min with a $\times$40 water-immersion objective (Fluor, NA 0.8W; Nikon). At the end of the 5 min period, fluorescence in the bleached cell was expressed as the percentage of recovery relative to the starting level just before photobleaching, a measure of the degree of GJ dye coupling. Cbx was included during the de-esterification period and was also present during the measurements.

Scrape loading and dye transfer. Cells were seeded in 4-well plates and grown to near confluency. They were then washed two times with nominally Ca^{2+}-free scrape loading and dye transfer (SLDT) buffer (137 mM NaCl, 5.36 mM KCl, 0.81 mM $MgCl_2 \cdot 6H_2O$, 5.55 mM D-glucose, 25 mM Hepes, pH 7.4), incubated for 1 min in SLDT buffer supplemented with the GJ-permeable tracer PI (1 mM) and a linear scratch was applied to the monolayer with a syringe needle. After 5 min, the dye was washed away with HBSS-Hepes and the cells were left for 15 min in HBSS-Hepes supplemented with 2 μg/ml Hoechst 33342 to allow the reporter dye to spread between cells *via* GJs and to stain the nuclei (all performed at room temperature). Images, 8 per well right next to the scrape, were acquired with a $\times$10 objective and the microscope as described for apoptosis detection. Gap junctional communication was quantified by counting the PI-positive nuclei and expressing them relative to the number of Hoechst-stained nuclei. Cbx was also present during the 15 min period after the linear scratch was made.

Oxidative stress measurements. Cells were loaded for 30 min with 10 μM CM-H_2DCFDA in HBSS-Hepes at room temperature, followed by a de-esterification period of 15 min. Subsequently cells were electroporated with 100 μM Cyt*C* and 100 μM DTR and kept in 200 μl culture medium. At defined time points, CM-H_2DCFDA fluorescence was measured with a plate reader (Victor-3, type 1420; Perkin-Elmer, Brussels, Belgium). Fluorescence values were corrected for background measurements (non-loaded cells) and normalized to control values (loaded with DTR-only).

Data and statistical analysis. Data are expressed as mean $\pm$ S.E.M., with '*n*' denoting the number of independent experiments. Multiple groups were compared by one-way ANOVA and a Bonferroni *post hoc* test using the GraphPad Instat software (Graphpad Software, San Diego, CA, USA). Statistical significance is indicated in the graphs by one symbol for $P<0.05$, two symbols for $P<0.01$ and three symbols for $P<0.001$.

Conflict of Interest

The authors declare no conflict of interest.

Acknowledgements. This work was impossible without the technical assistance of Ms Kirsten Leurs, Ms Anneleen Decock, Ms Marlies Bekaert, Ms Liesbeth Heyndrickx and Mr Eric Tack. We also gratefully acknowledge Mr Timothy Voorspoels for developing analysis tools and software. We thank Dr. D Boehning (Department of Neuroscience and Cell Biology, University of Texas Medical Branch, Galveston, TX, USA) for providing the IP3RCYT peptide. Our work is supported by: the Fund for Scientific Research Flanders (FWO-Vlaanderen), Belgium (G.0140.08, G.0134.09, G.0298.11N and WO.005.10N) and the Interuniversity Attraction Poles Program (Belgian Science Policy, project P6/31) assigned to LL; FWO (G.072810) assigned to DVK; a Methusalem grant (BOF09/01M00709) from the Flemish Government assigned to PV; FWO (G.0788.11N), the Research Council of the KU Leuven via OT START-1 (SRT/10/044) and the Interuniversity Attraction Poles Program (P6/28) assigned to GB; and the Interuniversity Attraction Poles Program (P6/28) assigned to CE.

1. Boehning D, van Rossum DB, Patterson RL, Snyder SH. A peptide inhibitor of cytochrome *c*/inositol 1,4,5-trisphosphate receptor binding blocks intrinsic and extrinsic cell death pathways. *Proc Natl Acad Sci USA* 2005; **102**: 1466–1471.
2. Verkhratsky A. Calcium and cell death. *Subcell Biochem* 2007; **45**: 465–480.
3. Decuypere JP, Monaco G, Bultynck G, Missiaen L, De Smedt H, Parys JB. The IP(3) receptor–mitochondria connection in apoptosis and autophagy. *Biochim Biophys Acta* 2011; **1813**: 1003–1013.
4. Sammels E, Parys JB, Missiaen L, De Smedt H, Bultynck G. Intracellular Ca^{2+} storage in health and disease: a dynamic equilibrium. *Cell Calcium* 2010; **47**: 297–314.
5. Szalai G, Krishnamurthy R, Hajnoczky G. Apoptosis driven by IP(3)-linked mitochondrial calcium signals. *EMBO J* 1999; **18**: 6349–6361.
6. Dupont G, Combettes L, Leybaert L. Calcium dynamics: spatio-temporal organization from the subcellular to the organ level. *Int Rev Cytol* 2007; **261**: 193–245.
7. Rong YP, Distelhorst CW. Bcl-2 protein family members: versatile regulators of calcium signaling in cell survival and apoptosis. *Annu Rev Physiol* 2008; **70**: 73–91.
8. Boitano S, Dirksen ER, Sanderson MJ. Intercellular propagation of calcium waves mediated by inositol trisphosphate. *Science* 1992; **258**: 292–295.
9. Saez JC, Berthoud VM, Branes MC, Martinez AD, Beyer EC. Plasma membrane channels formed by connexins: their regulation and functions. *Physiol Rev* 2003; **83**: 1359–1400.
10. Decrock E, Vinken M, De Vuyst E, Krysko DV, D'Herde K, Vanhaecke T *et al.* Connexin-related signaling in cell death: to live or let die? *Cell Death Differ* 2009; **16**: 524–536.
11. Decrock E, De Vuyst E, Vinken M, Van Moorhem M, Vranckx K, Wang N *et al.* Connexin 43 hemichannels contribute to the propagation of apoptotic cell death in a rat C6 glioma cell model. *Cell Death Differ* 2009; **16**: 151–163.
12. Cusato K, Bosco A, Rozental R, Guimaraes CA, Reese BE, Linden R *et al.* Gap junctions mediate bystander cell death in developing retina. *J Neurosci* 2003; **23**: 6413–6422.
13. Cusato K, Ripps H, Zakevicius J, Spray DC. Gap junctions remain open during cytochrome *c*-induced cell death: relationship of conductance to 'bystander' cell killing. *Cell Death Differ* 2006; **13**: 1707–1714.
14. Frank DK, Szymkowiak B, Josifovska-Chopra O, Nakashima T, Kinnally KW. Single-cell microinjection of cytochrome *c* can result in gap junction-mediated apoptotic cell death of bystander cells in head and neck cancer. *Head Neck* 2005; **27**: 794–800.
15. Udawatte C, Ripps H. The spread of apoptosis through gap-junctional channels in BHK cells transfected with Cx32. *Apoptosis* 2005; **10**: 1019–1029.
16. Peixoto PM, Ryu SY, Pruzansky DP, Kuriakose M, Gilmore A, Kinnally KW. Mitochondrial apoptosis is amplified through gap junctions. *Biochem Biophys Res Commun* 2009; **390**: 38–43.
17. Decrock E, Vinken M, Bol M, D'Herde K, Rogiers V, Vandenabeele P *et al.* Calcium and connexin-based intercellular communication, a deadly catch? *Cell Calcium* 2011; **50**: 310–321.
18. Allbritton NL, Meyer T, Stryer L. Range of messenger action of calcium ion and inositol 1,4,5-trisphosphate. *Science* 1992; **258**: 1812–1815.
19. Hofer T, Venance L, Giaume C. Control and plasticity of intercellular calcium waves in astrocytes: a modeling approach. *J Neurosci* 2002; **22**: 4850–4859.
20. Assefa Z, Bultynck G, Szlufcik K, Nadif Kasri N, Vermassen E, Goris J *et al.* Caspase-3-induced truncation of type 1 inositol trisphosphate receptor accelerates apoptotic cell death and induces inositol trisphosphate-independent calcium release during apoptosis. *J Biol Chem* 2004; **279**: 43227–43236.
21. Verbert L, Lee B, Kocks SL, Assefa Z, Parys JB, Missiaen L *et al.* Caspase-3-truncated type 1 inositol 1,4,5-trisphosphate receptor enhances intracellular Ca^{2+} leak and disturbs Ca^{2+} signalling. *Biol Cell* 2008; **100**: 39–49.
22. Huang DC, Adams JM, Cory S. The conserved N-terminal BH4 domain of Bcl-2 homologues is essential for inhibition of apoptosis and interaction with CED-4. *EMBO J* 1998; **17**: 1029–1039.
23. Rong YP, Bultynck G, Aromolaran AS, Zhong F, Parys JB, De Smedt H *et al.* The BH4 domain of Bcl-2 inhibits ER calcium release and apoptosis by binding the regulatory and coupling domain of the IP3 receptor. *Proc Natl Acad Sci USA* 2009; **106**: 14397–14402.
24. Monaco G, Decrock E, Akl H, Ponsaerts R, Vervliet T, Luyten T *et al.* Selective regulation of IP(3)-receptor-mediated Ca(2+) signaling and apoptosis by the BH4 domain of Bcl-2 versus Bcl-Xl. *Cell Death Differ* 2011; e-pub ahead of print 5 August 2011.
25. Bruzzone R, Veronesi V, Gomes D, Bicego M, Duval N, Marlin S *et al.* Loss-of-function and residual channel activity of connexin26 mutations associated with non-syndromic deafness. *FEBS Lett* 2003; **533**: 79–88.
26. Beltramello M, Piazza V, Bukauskas FF, Pozzan T, Mammano F. Impaired permeability to Ins(1,4,5)P3 in a mutant connexin underlies recessive hereditary deafness. *Nat Cell Biol* 2005; **7**: 63–69.
27. Anselmi F, Hernandez VH, Crispino G, Seydel A, Ortolano S, Roper SD *et al.* ATP release through connexin hemichannels and gap junction transfer of second messengers propagate Ca^{2+} signals across the inner ear. *Proc Natl Acad Sci USA* 2008; **105**: 18770–18775.
28. Nutt LK, Chandra J, Pataer A, Fang B, Roth JA, Swisher SG *et al.* Bax-mediated Ca^{2+} mobilization promotes cytochrome *c* release during apoptosis. *J Biol Chem* 2002; **277**: 20301–20308.
29. Peng TI, Jou MJ. Oxidative stress caused by mitochondrial calcium overload. *Ann N Y Acad Sci* 2010; **1201**: 183–188.
30. Tang EH, Vanhoutte PM. Gap junction inhibitors reduce endothelium-dependent contractions in the aorta of spontaneously hypertensive rats. *J Pharmacol Exp Ther* 2008; **327**: 148–153.
31. Dupont G, Koukoui O, Clair C, Erneux C, Swillens S, Combettes L. Ca^{2+} oscillations in hepatocytes do not require the modulation of InsP3 3-kinase activity by Ca^{2+}. *FEBS Lett* 2003; **534**: 101–105.
32. De Smedt F, Verjans B, Mailleux P, Erneux C. Cloning and expression of human brain type I inositol 1,4,5-trisphosphate 5-phosphatase. High levels of mRNA in cerebellar Purkinje cells. *FEBS Lett* 1994; **347**: 69–72.
33. Morales AP, Carvalho AC, Monteforte PT, Hirata H, Han SW, Hsu YT *et al.* Endoplasmic reticulum calcium release engages Bax translocation in cortical astrocytes. *Neurochem Res* 2011; **36**: 829–838.
34. Peixoto PM, Lue JK, Ryu SY, Wroble BN, Sible JC, Kinnally KW. Mitochondrial apoptosis-induced channel (MAC) function triggers a Bax/Bak-dependent bystander effect. *Am J Pathol* 2011; **178**: 48–54.
35. Scorrano L, Oakes SA, Opferman JT, Cheng EH, Sorcinelli MD, Pozzan T *et al.* BAX and BAK regulation of endoplasmic reticulum Ca^{2+}: a control point for apoptosis. *Science (New York, NY)* 2003; **300**: 135–139.
36. Carvalho AC, Sharpe J, Rosenstock TR, Teles AF, Youle RJ, Smaili SS. Bax affects intracellular Ca^{2+} stores and induces Ca^{2+} wave propagation. *Cell Death Differ* 2004; **11**: 1265–1276.
37. Oakes SA, Scorrano L, Opferman JT, Bassik MC, Nishino M, Pozzan T *et al.* Proapoptotic BAX and BAK regulate the type 1 inositol trisphosphate receptor and calcium leak from the endoplasmic reticulum. *Proce Natl Acad Sci USA* 2005; **102**: 105–110.
38. Niessen H, Harz H, Bedner P, Kramer K, Willecke K. Selective permeability of different connexin channels to the second messenger inositol 1,4,5-trisphosphate. *J Cell Sci* 2000; **113** (Part 8): 1365–1372.
39. Baumgartner HK, Gerasimenko JV, Thorne C, Ferdek P, Pozzan T, Tepikin AV *et al.* Calcium elevation in mitochondria is the main Ca^{2+} requirement for mitochondrial permeability transition pore (mPTP) opening. *J Biol Chem* 2009; **284**: 20796–20803.
40. Sims CE, Allbritton NL. Metabolism of inositol 1,4,5-trisphosphate and inositol 1,3,4,5-tetrakisphosphate by the oocytes of *Xenopus laevis*. *J Biol Chem* 1998; **273**: 4052–4058.